ELECTROMAGNETIC MODELING

Numerical modeling of electromagnetic (EM) fields or *computational electromagnetics* is a combination of numerical methods and field theory—a discipline in its own right and of growing importance in such diverse areas as microwave and RF (radio frequency) engineering, antenna design, EM field scattering, semiconductor physics, bioelectromagnetics, and electromagnetic compatibility and interference (EMC/EMI).

The starting point for modeling electromagnetic fields is Maxwell's equations considering a set of known boundary/initial conditions. In addition, certain theorems and principles, such as superposition, equivalence, and duality can be utilized. Entirely analytical solutions to Maxwell's equations are possible only for a narrow range of problems and most of them were solved a long time ago. Classical analytical methods are the methods of separation of variables, conformal mapping, series expansion, and integral methods (if the integrals have analytical solutions).

Today's complexity of relevant EM field problems prevent entirely analytical (closed-form) solutions to Maxwell's equations. Rather, numerical approaches are necessary which approximate the exact solution with any desired degree of accuracy. Does this eliminate the need for analytical methods? Certainly not! In fact, analytical preprocessing is part of all numerical methods, and if the analytical content is high, the method is often described as semi-analytical.

In general, the electromagnetic field problem can be conveniently formulated as partial differential equation while that of the source problem as integral equation (operator equation). The objective of numerical methods is to transform an exact operator equation into a solvable (discrete) matrix equation. To achieve this, virtually all numerical methods follow the same principle steps: First, to express the unknown function of the operator equation by a sum of linear independent functions with unknown expansion coefficients. This is often called a trial function which approximates the real function if the number of terms in the sums goes to infinity. Second, the continuous solution domain is represented by a set of discretized subdomains consisting of a finite number of elements or nodes. Third, to determine the unknown expansion coefficients in the trial function, some form of error minimization is chosen. Employing either variational principles or the method of weighted residuals, the operator equation is transformed into a matrix equation which must be solved by appropriate techniques.

Depending on the kind of operator used, numerical methods are in general categorized into domain methods and boundary methods. More recently a new category has been added, that of hybrid methods.

Domain methods solve the electromagnetic field problem described by partial differential equations. Examples are the finite difference method and the finite element method. Both methods are based on differential equations and on discretization of the entire computational domain. *Boundary methods* solve the electromagnetic source problem described by integral equations, either volume integral equations or boundary integral equations. Examples are the boundary element method or the method of moments. The latter can also be used to solve differential equations. *Hybrid methods* are a combination of two or more different methods. A hybrid numerical approach can be a two-step procedure or an implicit hybrid algorithm. In the two-step procedure, one part of the problem is solved with one method, the results of which become the input parameters for the next method. In the implicit hybrid algorithm two or more modeling approaches are combined into one new algorithm to exploit only the advantageous features of each method. Hybrid methods are very useful for problems that can either not be solved within the framework of a single technique or in cases where a combination of methods results in a computationally more efficient algorithm to model the electromagnetic field.

Over the last twenty years the importance of modeling electromagnetic fields has increased manifold. This refers not only to the analysis of arbitrary electromagnetic field problems but also to the CAD (computer-aided design) of circuits and components. With rising operating frequency and higher circuit density, quasi-static analysis methods are replaced by full-wave analysis methods to account for near-field effects or higher order mode interaction. Simplifying assumptions about material properties have been replaced by realistic material descriptions taking dispersion and losses into account. With the steady increase in computer power, research in electromagnetic modeling is still advancing at a rapid pace, intro-

ducing new techniques, expanding the capability of existing methods or simply improving their computational efficiency and accuracy. Only some of the multitude of electromagnetic modeling techniques available today can be outlined here.

This article will focus only on some mainstream techniques, most of which employ either the method of weighted residuals or variational principles. We will begin with modeling techniques in the frequency domain, most importantly the method of moments (MOM). This section is followed by time-domain methods and here in particular the finite-difference time-domain method (FDTD) and the transmission line matrix (TLM) method. Finally, a brief overview with respect to hybrid methods concludes this article. A comparison between the various modeling approaches as well as their advantages and disadvantages is added where appropriate.

For a more detailed representation of the various methods, the interested reader is referred to the books by Sadiku (1) or Zhou (2). Another excellent source of information is the book edited by Itoh (3) which discusses the various methods in the context of passive microwave circuit modeling.

FREQUENCY DOMAIN METHODS

Most electromagnetic modeling techniques operate in the frequency domain, that is, the time derivative d/dt is replaced by $j\omega t$. Therefore, all calculations are performed at a single frequency only. In cases where the electromagnetic field is of interest over a frequency band, repeated calculations are necessary. This is in contrast to time-domain methods. Here a single run of the algorithm, after a proper impulse excitation, followed by a Fourier transform of the impulse response, provides the information over a wide frequency range. Which method to use depends on the problem at hand.

The Method of Moments

The *method of moments* (MOM) is a general form of weighted residuals to solve integral, differential, and integro-differential equations. The method itself does not provide any information about the derivation of the governing equation, thereby allowing its applicability to a wide range of physical phenomena.

The equations solved by MOM are normally an electric field integral equation (EFIE) or a magnetic field integral equation (MFIE) of the following form

$$\text{EFIE:} \quad \mathbf{E} = f_{\mathrm{e}}(\mathbf{J})$$
$$\text{MFIE:} \quad \mathbf{H} = f_{\mathrm{m}}(\mathbf{J})$$

whereby $\mathbf{E}$ and $\mathbf{H}$ are the incident field quantities and $\mathbf{J}$ is the induced current density. The form of integral equation (EFIE or MFIE) depends on the problem. In most cases these integrals are formulated in the frequency domain although the MOM can also be applied to solve problems in the time domain.

The MOM as a mathematical technique was first introduced by Mikhlin (4) and later popularized in the area of numerical electromagnetics by Harrington (5).The mathematical formulation of the MOM is simple and general. Consider a linear operator L such that

$$L\boldsymbol{J} = \boldsymbol{g} \tag{1}$$

The function $\boldsymbol{J}$ (e.g., current density) is the response of the system represented by the operator L to the excitation $\boldsymbol{g}$ (magnetic or electric field). When L and $\boldsymbol{g}$ are known, Eq. (1) represents an analysis problem from which $\boldsymbol{J}$ is determined. A synthesis problem is one in which both $\boldsymbol{J}$ and $\boldsymbol{g}$ are known but L is to be determined.

The MOM solution of Eq. (1) takes advantage of the linearity of the operator L to expand $\boldsymbol{J}$ in a series of the form

$$\boldsymbol{J} = \sum_m a_m \boldsymbol{J}_m \tag{2}$$

The a_m's are unknown expansion coefficients and the $\boldsymbol{J}_m$'s are known functions in the domain of the operator L. The functions $\boldsymbol{J}_m$, which are assumed to form a complete set, are called basis functions. Substituting the expansion of $\boldsymbol{J}$ in Eq. (1) and using the linearity of L, we get

$$L\boldsymbol{J} = L\sum_m a_m \boldsymbol{J}_m = \sum_m a_m L\boldsymbol{J}_m = \boldsymbol{g} \tag{3}$$

The original problem is now reduced to determining the expansion coefficients from this last equation. In the MOM, both sides of the equation are projected onto the range of the operator L. Let $\boldsymbol{T}_m$ denote a complete set of functions in the range of L. The $\boldsymbol{T}_m$'s are referred to as testing or weighting functions. Taking the inner product of Eq. (3) against the testing functions, yields

$$\sum_m a_m \langle \boldsymbol{T}_n, L\boldsymbol{J}_m \rangle = \langle \boldsymbol{T}_n, \boldsymbol{g} \rangle, \qquad n = 1, 2, \ldots \tag{4}$$

Here, a suitable inner product (a linear form) is assumed to be known. Usually, the inner product is taken as the integral of the product of the arguments

$$\langle \boldsymbol{J}, \boldsymbol{g} \rangle = \int \boldsymbol{J}\boldsymbol{g} \tag{5}$$

Equation (4) can be rewritten in a more convenient matrix form

$$[A][a] = [U] \tag{6}$$

where

$$[A]_{mn} = \langle \boldsymbol{T}_m, L\boldsymbol{J}_n \rangle \tag{7}$$

$$[U]_m = \langle \boldsymbol{T}_m, \boldsymbol{g} \rangle \tag{8}$$

If the matrix $[A]$ is not singular, its inverse $[A]^{-1}$ exists. The expansion coefficients a_m are then given by

$$[a] = [A]^{-1}[U] \tag{9}$$

Once the expansion coefficients are known, the solution is given by Eq. (2). The MOM is most commonly implemented in the form of Galerkin's method in which the testing functions are equal to the basis functions, $\boldsymbol{T}_m = \boldsymbol{J}_m$.

In practice, the infinite expansion Eq. (2) is truncated at some upper value of m. The approximate solution, given by Eq. (9), is then straightforwardly computed using a computer. The efficiency of the technique depends heavily on having basis functions which approximate well the exact solution with

only a few terms. Therefore, MOM techniques are not very effective in the analysis of complex geometries or inhomogeneous dielectrics. On the other hand, MOM techniques are particularly efficient for the analysis of antennas and electromagnetic scattering problems.

The Mode Matching Technique

The mode matching technique (MMT), or modal analysis method, can be viewed as a special case of the method of moments and is a frequently used analysis tool for scattering of electromagnetic waves at metal waveguide discontinuities. In this method, the fields immediately left and right from the discontinuity are expanded in a series of weighted eigenfunctions. From the matching condition or continuity condition of the fields tangential to the discontinuity plane the coefficients of the series expansions can be determined. Details of the method can be found in Refs. 6 and 7. The MMT has been successfully applied to eigenvalue as well as to scattering problems both in homogeneous waveguides as well as partially dielectric loaded waveguides. Numerous application examples for eigenvalue problems are given, for example, in Refs. 8 and 9 and for scattering problems in Refs. 10 and 11.

The basic problem to be solved in the MMT is to find the coefficients of the field expansion to minimize the least square error between the exact EM field and the approximating series of eigenfunctions. If we postulate $g(x)$ as the exact field in the aperture between two subregions, the approximation by a series of orthogonal eigenfunctions $f_i(x)$ is written

$$g(x) \cong \sum_i^N a_i f_i(x), \qquad x \in x_1, x_2 \tag{10}$$

where a_i denote the weighting (expansion) coefficients. By multiplying both sides of Eq. (10) with a set of weighting functions, $w_j(x)$, and integrate over the domain of x results in

$$\int_{x_1}^{x_2} w_j(x) g(x)\, dx = \sum_i^N a_i \int_{x_1}^{x_2} w_{ji}(x) f_i(x)\, dx \tag{11}$$

We solve Eq. (11) such that its weighted residual is zero:

$$\int_{x_1}^{x_2} w_j(x) \left[g(x) - \sum_i^N a_i f_i(x)\, dx \right] dx = 0, \quad j = 1, 2, \ldots \mathrm{N} \tag{12}$$

If the weighting function is a set of delta functions

$$w_j(x) = \delta(x - x_j)$$

Eq. (10) becomes Eq. (13) which is known as point matching Eq. (11)

$$g(x_j) \cong \sum_i^N a_i f_i(x_j), \quad j = 1, 2, \ldots N \tag{13}$$

Eq. (13) is solved for the a_i's. If the weighting functions are the eigen-functions themselves, we use the least square error to select the expansion coefficients such as to minimize the integrated squared error

$$0 = \frac{\partial}{\partial a_i} \int \left[g(x) - \sum_i^N a_i f_i(x) \right]^2 dx$$

By using the orthogonality of the eigenfunctions $f_i(x)$ we find the individual coefficients

$$\frac{\int_{x_1}^{x_2} f_i(x) g(x)\, dx}{\int_{x_1}^{x_2} f_i(x)^2\, dx} = a_i \tag{14}$$

It should be noted that the integral in the denominator of Eq. (14) is a normalization constant while the integral in the numerator (the coupling integral) can in most cases be solved analytically, except in cases where the geometry of the regions left and right of a discontinuity is described by different coordinate systems.

The MMT becomes a powerful analysis tool in conjunction with the generalized scattering matrix approach (GSM). The GSM relates all reflected wave amplitudes of fundamental and higher order modes at discontinuities to the incident wave amplitudes. Wave amplitudes are in this context the power normalized expansion coefficients in Eq. (10).

A simple example illustrates the MMT in conjunction with the GSM technique. A waveguide step discontinuity is shown in Fig. 1. We assume that in both waveguide sections only the fundamental TE_{10} mode can propagate.

The TE_{10} mode consists of three field components of which two, E_y and H_x, are tangential to the discontinuity plane at $z = 0$ [Fig. 1(b)]. In region 1 and 2, the electric field component can be expressed as a series of eigenfunctions such as in Eq. (10). Applying the continuity condition at the discontinuity plane ($z = 0$), $E_y^1 = E_y^2$, results in

$$\sum_{m=1}^{M} T_m^1 \sin\left(\frac{m\pi}{a} x\right) (A_m^1 + B_m^1) = \sum_{n=1}^{N} T_n^2 \sin\left(\frac{n\pi}{a - x_1}(x - x_1)\right) (A_n^2 + B_n^2) \tag{15}$$

The coefficients T in Eq. (15) ensure power normalization of the incident, A, and reflected, B, wave amplitudes for fundamental and higher order modes. The products $\mathrm{T} \cdot \mathrm{A}$ or $\mathrm{T} \cdot \mathrm{B}$ are the expansion coefficients of Eq. (10). Multiplying both sides of Eq. (15) with $\sin(i\pi/a\ x)$ and integrating over the

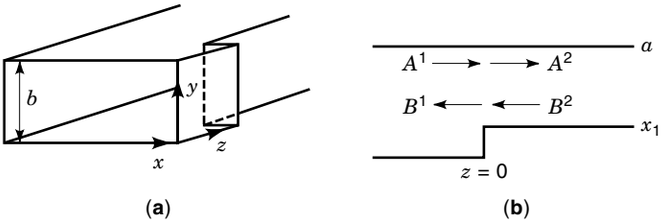

Figure 1. *H*-plane discontinuity in rectangular waveguide. (a) Perspective view; (b) Scattered wave amplitudes.

cross-section $x = 0-a$ yields

$$Ey\colon A_i^1 + B_i^1 = \underbrace{\frac{\sum_{n=1}^{N} T_n^2 \int_{x_1}^{a} \sin\left(\frac{n\pi}{a}x\right) \sin\left(\frac{i\pi}{a-x_1}(x-x_1)\right) dx}{\int_0^a \sin^2\left(\frac{i\pi}{a}x\right) dx}}_{LE} (A_n^2 + B_n^2) \quad (16)$$

The normal modes satisfy the orthogonality relation and the integral in the denominator of Eq. (16) thus becomes

$$\int_0^a \sin^2\left(\frac{i\pi}{a}x\right) dx = \frac{a}{2} \quad (17)$$

A similar equation is obtained from the continuity condition of the H_x-component

$$H_x\colon \underbrace{\frac{\sum_{m=1}^{M} T_m^2 Y_m \int_{x_1}^{a} \sin\left(\frac{m\pi}{a}x\right) \sin\left(\frac{i\pi}{a-x_1}(x-x_1)\right) dx}{\int_{x_1}^{a} \sin^2\left(\frac{i\pi}{a-x_1}x - x_1\right) dx}}_{LH} A_i^1 - B_i^1 = A_m^2 - B_m^2 \quad (18)$$

Both equations can be written in matrix notation

$$\begin{aligned} E_y\colon &\quad [A]^1 + [B]^1 = [L_E] \cdot ([A]^2 + [B]^2) \\ H_x\colon &\quad [L_H] \cdot ([A]^1 - [B]^1) = [A]^2 - [B]^2 \end{aligned}$$

Rearranging these equations leads to the generalized scattering matrix of the waveguide discontinuity

$$\begin{bmatrix} [B]^1 \\ [A]^2 \end{bmatrix} = \begin{bmatrix} [S_{11}] & [S_{12}] \\ [S_{21}] & [S_{22}] \end{bmatrix} \begin{bmatrix} [A]^1 \\ [B]^2 \end{bmatrix} \quad (19)$$

A well-known problem in the MMT is the slow convergence rate and the relative convergence phenomenon. The latter can be alleviated to some degree by choosing the number of modes on both sides of the discontinuity in the same ratio as the waveguide dimensions left and right from the discontinuity. The MMT is also not well suited for problems in which the structure contains a mixed coordinate system. Coupling integrals must then be solved numerically which makes the algorithm slow and not very effective. In those cases the MMT can be combined with other techniques (hybrid methods discussed later) which are more appropriate for certain parts of the problem.

Coupled Integral Equation Technique

The problem of slow convergence in the MMT is due mainly to the fact that the eigenfunctions of the waveguides left and right from the discontinuity do not accommodate the boundary conditions of the fields in the discontinuity plane. This is not so in the coupled integral equation technique (CIET). A major advantage of the CIET is its ability to include a priori information, such as the edge conditions, at multiple discontinuities simultaneously. The salient features of the technique can be found in Refs. 12 and 13; here we only show how the edge condition at a single discontinuity is handled through the CIET. For this we refer again to the example of Fig. 1.

The tangential electric field within the discontinuity region (the gap region) is expanded in a series of basic functions which are chosen such that they include the edge condition of the electric field at $x = x_1$

$$E_{\text{gap}}(x) = \sum_i^I c_i E_i(x) \begin{cases} E_{\text{gap}} = 0, & 0 \le x \le x_1 \\ E_{\text{gap}} \ne 0, & x_1 < x \le a \end{cases} \quad (20)$$

A possible set of basic functions that satisfy the edge condition is the following

$$E_i(x) = \frac{\sin\left[\frac{i\pi}{a-x_1}(x-x_1)\right]}{[(x-x_1)(2a-x_1-x)]^{1/3}}$$

Matching the tangential electric field of both regions (1 and 2) to the electric field in the discontinuity plane, E_{gap}, yields

$$\begin{aligned} E_y^1(x) &= E_{\text{gap}}(x), \qquad 0 \le x \le a \\ E_y^2(x) &= E_{\text{gap}}(x), \qquad x_1 \le x \le a \end{aligned} \quad (21)$$

From Eq. (21), using Eq. (20), one obtains

$$\begin{aligned} B_i^1 &= -\delta_{i1} + \frac{2}{a}\int_{x_1}^{a} E_{\text{gap}}(x) \sin\left(\frac{i\pi}{a}x\right) dx \\ B_i^2 &= \frac{2}{a-x_1}\int_{x_1}^{a} E_{\text{gap}}(x) \sin\left(\frac{i\pi}{a-x_1}x - x_1\right) dx \end{aligned} \quad (22)$$

Utilizing the matching condition from the tangential magnetic field, $H_x^1 = H_x^2$, which is defined in the interval $x_1 \le x \le a$ and replacing the expansion coefficients therein by using Eq. (22), leads to the following integral equation

$$\begin{aligned} 2Y_1^1 \sin\left(\frac{\pi}{a}x\right) = \sum_i Y_i^2 \frac{2}{a-x_1}\int_{x_1}^{a} E_{\text{gap}}(x) \sin\left(\frac{i\pi}{a-x_1}x' - x_1\right) \\ \sin\left(\frac{i\pi}{a-x_1}x - x_1\right) dx' + \sum_n Y_n^1 \frac{2}{a}\int_{x_1}^{a} E_{\text{gap}}(x) \\ \sin\left(\frac{n\pi}{a}x'\right) \sin\left(\frac{n\pi}{a}x\right) dx' \end{aligned} \quad (23)$$

The remaining step is to find the expansion coefficients c_i in Eq. (20). This is accomplished by substituting Eq. (20) in Eq. (23) and using the method of moments in the form of Galerkin's method. The number of terms in Eq. (20), the value of I, is increased until convergence is achieved. Typically only a few terms are needed to accurately describe the discontinuity. Although the analytical content of the CIET is higher than for the MMT, the numerical efficiency is significantly better and no relative convergence problems are encountered.

The Spectral Domain Method

The spectral domain method (SDM) (14) utilizes the Fourier transformation to eliminate all but one space variable in the Helmholtz equation. The latter is then solved analytically for the remaining space variable. The SDM is a computationally very efficient analysis tool for microwave transmission lines.

The method has found numerous applications, mainly in the analysis of electromagnetic fields in planar transmission line structures where the overall cross-section can be divided into homogeneous dielectric subregions. Although the method was originally introduced for single conductor transmission lines with infinitely thin conductor (15), the SDM has been generalized recently [i.e., (16,17)] to include also finite metallization thickness and multiple dielectric layers.

The method is best illustrated by considering the example of a microstrip line (Fig. 2). In regions with constant μ and ϵ the electromagnetic field, represented by a potential function $\phi^{e,h}$, satisfies the Helmholtz equation

$$\left(\frac{\partial}{\partial x^2}+\frac{\partial}{\partial y^2}+\frac{\partial}{\partial z^2}+k^2\right)\phi^{e,h}(x,y,z)=0$$

A two-dimensional Fourier transform on $\phi^{e,h}$ (for example on x and z)

$$\tilde{\phi}^{e,h}(\alpha,y,\beta)=\int\int e^{-j(\alpha x+\beta z)}\phi^{e,h}(x,y,z)\,dx\,dz \tag{24}$$

transforms the Helmholtz equation into one that contains only one space variable

$$\frac{\partial^2\tilde{\phi}^{e,h}}{\partial y^2}-(\alpha^2+\beta^2-k^2)\tilde{\phi}^{e,h}=0 \tag{25}$$

A solution to this equation is known in the form of exponential functions or hyperbolic functions. In each homogeneous subregion, $\phi^{e,h}$ can thus be transformed from one boundary to the opposite. With respect to Fig. 2, this implies that the known boundary condition of the electromagnetic field at planes $y = 0$ and $y = h$ can be transformed into plane $y = d$. The final step in the formulation of the SDM is then to satisfy the boundary condition of the tangential fields at the interface $y = d$, which are in the transformed domain

$$\tilde{E}_{z1}=\tilde{E}_{z2};\ \tilde{E}_{x1}=\tilde{E}_{x2};\ \tilde{H}_{x2}-\tilde{H}_{x1}=\tilde{J}_z;\ \tilde{H}_{z2}-\tilde{H}_{z1}=-\tilde{J}_x$$

$\tilde{J}_x$ and $\tilde{J}_z$ are the Fourier transforms of the unknown currents on the strip. From this, a matrix equation can be derived as follows

$$\begin{bmatrix}\tilde{E}_{z1}\\ \tilde{E}_{x1}\end{bmatrix}=\begin{bmatrix}\tilde{Z}_{zz}\tilde{Z}_{zx}\\ \tilde{Z}_{xz}\tilde{Z}_{xx}\end{bmatrix}\begin{bmatrix}\tilde{J}_z\\ \tilde{J}_x\end{bmatrix} \tag{26}$$

with $\tilde{J}_z=\sum_m^M c_m\tilde{J}_{zm}(\alpha)$ and $\tilde{J}_x=\sum_m^N d_m\tilde{J}_{xm}(\alpha)$.

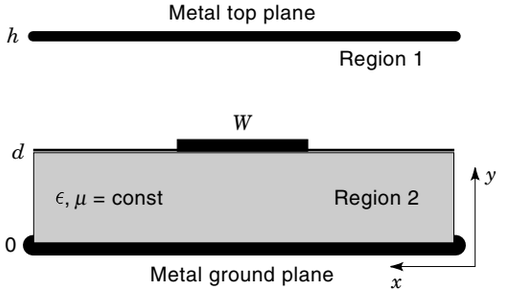

Figure 2. Cross section of a microstrip transmission line.

Using Galerkin's technique, $\tilde{E}_x$ and $\tilde{E}_z$ in Eq. (26) can be eliminated and a matrix equation for the expansion coefficients c_m and d_m is found

$$\underbrace{\begin{bmatrix}\int_\alpha \tilde{J}_z\tilde{Z}_{zz}\tilde{J}_z & \int_\alpha \tilde{J}_z\tilde{Z}_{zx}\tilde{J}_x\\ \int_\alpha \tilde{J}_x\tilde{Z}_{xz}\tilde{J}_z & \int_\alpha \tilde{J}_1\tilde{Z}_{xx}\tilde{J}_x\end{bmatrix}}_{[A]}\begin{bmatrix}c\\ d\end{bmatrix}=0 \tag{27}$$

The propagation constant β is contained in the matrix elements of $\tilde{Z}$. The transformed currents on the strip are found from an educated guess of the current distribution on the strip in the space domain. To describe the current in the space domain as accurate as possible, basis functions must be employed that are zero outside the strip area and also model the singular behaviour of the magnetic field components normal to the strip edge. Equation (27) can then be solved for β by finding the zeros of the determinant of $[A]$ (i.e., $\det[A] = 0$).

A disadvantage of the SDM is that the algorithm is developed for very specific transmission line geometries. If the geometry changes, for example, substrate regions become inhomogeneous, or conductor contours do not fit into a rectangular coordinate system, the SDM algorithm must be reformulated. This applies also to the previous methods and can only be avoided if more general methods are utilized that are based on finite element or finite difference discretization of Maxwell's equations or the Helmholtz equation.

The Generalized Multipole Method

The generalized multipole technique (GMT) is also based on the weighted residual technique. It is a unique form of the method of moments in that the expansion functions are analytic solutions of the fields generated by sources a distance away from the surface where the boundary condition is being enforced. The GMT is a frequency domain method for calculating electromagnetic fields both in 2-D and in 3-D. The method is also known as the multiple multipole method [(MMP) (19)]. In the GMT the field domain is separated into a number of subdomains D_i, each with linear and homogeneous material. In each D_i, a separate expansion of the electromagnetic field is given as

$$\begin{pmatrix}E\\ H\end{pmatrix}=\begin{pmatrix}E_0\\ H_0\end{pmatrix}+\sum_{l=1}^{\infty}a_l\begin{pmatrix}E_l\\ H_l\end{pmatrix} \tag{28}$$

In static cases, either the electric or magnetic field is replaced by a potential. E_0, H_0 in Eq. (28) is a given excitation. Any choice of the unknown coefficients a_l results in a correct solution of Maxwell's equation, since E_l and H_l is such a solution. Thus, all degrees of freedom in this solution, that is, the set a_l, may be used to satisfy the boundary conditions. The GMT is often referred to as a semi-analytical method since the differential equations (i.e., Maxwell's equations) in each subdomain D_i are solved analytically (= exactly), while the boundary conditions on the boundaries ∂D_{ij} between subdomains D_i and D_j are solved numerically (= approximately). In order to accelerate convergence and to keep the number of unknowns as low as possible, the expansion in each subdomain D_i is chosen such that it fits best to the particular shape of D_i and the particular excitation.

The boundary conditions are fulfilled numerically (approximately), using the extended point matching technique. This is numerically equivalent to both a projection technique using Galerkin's choice of test functions and a least squares error minimization. All the boundary conditions concerning fields may be taken into account. As a special case, surface impedance boundary conditions are also possible. Also in the GMT/MMP, a system of linear equations is developed which is solved for the best coefficients of the expansion functions. In order to save computer memory and to improve the numerical stability, matrix solvers like Givens plane rotation may be used.

The difference between the GMT and the MOM is that the latter normally employs expansion functions which are located on the boundary representing quantities such as charge or current. The fields are then determined by integrating these quantities over the entire surface. This integration is not necessary in the GMT since the expansion functions are already field solutions corresponding to multiple poles.

Dielectric and conducting boundaries are treated with the same efficiency in the GMT because the same expansion functions are used. Therefore, GMT models are quite general and do not suffer from the limitations of most MOM models. On the other hand, MOM models that employ functions optimized for a particular problem, are generally more efficient than GMT models.

An overview article about GMT was published by Ludwig (18). Details of the GMT and application examples are given in the text by Hafner (19) and Leuchtmann (20).

The Method of Lines

The method of lines (MOL) is also a semianalytical method which was developed by Russian mathematicians (21,22) to solve partial differential equations. In this scheme a set of coupled differential equations is transformed into a set of ordinary differential equations which can be solved analytically. As such the MOL can also be classified as a hybrid method since it combines an analytical approach with the finite difference method. For the microwave domain, Pregla and co-workers were the first to adopt this method, mainly for the analysis of planar microwave circuits. A very detailed description of the method is given by Pregla and Pascher in Ref. 23. The MOL provides, in comparison to the MMT or the SDM, more flexibility in the analysis of transmission line geometries with almost arbitrary cross section. The only restriction is that at least one space direction must be amenable to an analytical solution, which is always true for planar transmission lines.

To illustrate the MOL, it is best to choose a two-dimensional problem, although three-dimensional problems can be solved as well. An example of a cross section suitable for an MOL analysis is again the microstrip line as shown in Fig. 2, only this time we consider also the finite metallization thickness. The objective is to find the effective permittivity, ϵ_{eff}. Assuming a symmetrical structure, the domain is bounded with a magnetic wall at the symmetry plane, and with electric walls elsewhere. The discretization of the cross section by lines is shown in Fig. 3 with 3 homogeneous subdomains. In each subregion the wave equation is discretized in x-direction with step size h, and analytical solutions are sought in y-direction along the solid and dashed lines shown in the figure. To be more precise, analytical solutions for the electric field

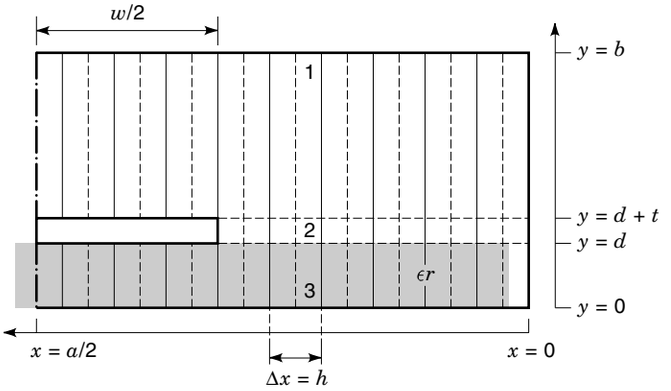

Figure 3. Discretization scheme of the method of lines for a microstrip transmission line with metallic enclosure of dimensions $a \times b$.

components are defined on the solid lines ($x = kh$, $k = 0, 1, 2, \ldots$) in order to fulfill the Dirichlet boundary condition at $x = 0$ by setting $E_{tangential} = 0$. The magnetic field will be defined on the dashed lines ($x = kh + h/2$, $k = 0, 1, 2, \ldots$), where the Neumann boundary condition at $x = 0$ can be fulfilled to a first order [$H_{tangential}(+h/2) = H_{tangential}(-h/2)$]. Similar considerations apply to the magnetic wall boundary at $x = a/2$, as well as to subdomain 2 besides the strip. The discretization in x-direction is done by a finite difference scheme, and the second-order derivative at line i can be written as

$$\left.\frac{\partial^2\phi}{\partial x^2}\right|^i \approx \frac{\phi^{i-1} - 2\phi^i + \phi^{i+1}}{h^2}$$

The coupled differential equations in each subregion are then found in matrix form as

$$\frac{\partial^2 \boldsymbol{\phi}}{\partial y^2} - \frac{1}{h^2}[P]\boldsymbol{\phi} + k_c^2 \boldsymbol{\phi} = 0 \tag{29}$$

whereby the vector $\boldsymbol{\phi}$ represents either the longitudinal electric (E_z) or magnetic (H_z) field component. The second-order difference operator [P] couples the differential equations of three neighboring lines. Because matrix [P] is symmetric, decoupling of the above differential equations is possible by an orthogonal transformation matrix [T] ($[T]^{-1} = [T]^t$) such that

$$\overline{\boldsymbol{\phi}} = [T]^t \boldsymbol{\phi}$$

The eigenvectors of [P] are the columns of [T]. The discretized wave equations in the transformed domain is decoupled and written as

$$\frac{\partial^2 \overline{\boldsymbol{\phi}}}{\partial y^2} + \left(k_c^2 - \left(\frac{\lambda_k}{h}\right)^2\right)\overline{\boldsymbol{\phi}} = 0 \tag{30}$$

where λ_k^2 are the eigenvalues of [P]. Equation (30) can now be solved analytically along each line by using trigonometric functions. In other words, the EM fields in the transformed domain can be transformed from one boundary of a subregion to the opposite. At the interfaces between subregions (i.e., at $y = d$ and at $y = d + t$, Fig. 3), the tangential fields are matched at the points where the lines cross the interface

planes. Depending on the problem at hand, field matching is done either in the transformed domain or in the space domain. The latter requires full matrix inversions, which complicates the algorithm. Regarding the example of the microstrip line, field matching in the space domain becomes necessary due to the finite thickness of the strip (i.e., the number of lines to match is different from one subregion to another). The assumption of an infinitely thin strip would make possible a field matching in the transformed domain and, therefore, lower the computational cost of the algorithm by avoiding several matrix inversions. In any case, an eigenvalue problem must be solved for k_c. The size of the eigenvalue matrix corresponds to the minimum number of lines in one layer, i.e., the number of lines in region 2 besides the strip. The effective permittivity of the microstrip line is then found from the wavenumber k_c.

A significant advantage of the MOL over other space discretization methods like the finite difference method or the finite element method is that a two-dimensional problem requires only a one-dimensional space discretization. This feature can lower the computational requirements significantly at the cost of a higher analytical content.

The Finite-Difference Method

The finite-difference method (FDM) is an approximate method to solve partial differential equations. In contrast to the method of lines, the computational domain is discretized in all three space directions. The derivative operations, for example for the space variable x, $\partial\phi/\partial \mathrm{x}$ and $\partial^2\phi/\partial \mathrm{x}^2$ are approximated by $\Delta\phi(x)/\Delta x$ and $\Delta^2\phi(x)/\Delta x^2$ and thus the partial differential equation is reduced to a set of algebraic equations. In electromagnetics as in other areas of engineering, the FDM is one of the most important methods to solve a wide range of problems. These include linear and nonlinear problems, time and frequency domain problems, wave propagation in homogeneous and inhomogeneous media and in media with different boundary conditions. An early example on the application of the FDM to waveguide problems is given in Refs. 25 and 26. Detailed chapters on the FDM can be found in books by Sadiku and Zhou (1,2).

To illustrate the FDM, we choose a problem that can be described by the two-dimensional Laplace equation

$$\frac{\partial^2\phi}{\partial \mathrm{x}^2} + \frac{\partial^2\phi}{\partial \mathrm{y}^2} = 0 \tag{31}$$

Sampling the continuous electromagnetic field in the computational domain by a mesh of regular points separated by a constant distance h (Fig. 4), Eq. (31) is approximated by the difference quotients at the adjacent mesh points. Depending on the choice of the difference and the difference quotient, different methods can be used to derive the discretization formulations. Using a Taylor expansion, the potentials surrounding the center node o (Fig. 4) can be expressed as

$$\begin{aligned}
\phi_{x-h} &= \phi_O - h\left(\frac{\partial\phi}{\partial \mathrm{x}}\right)_O + \frac{h^2}{2!}\left(\frac{\partial^2\phi}{\partial \mathrm{x}^2}\right)_O - \frac{h^3}{3!}\left(\frac{\partial^3\phi}{\partial \mathrm{x}^3}\right)_O + \epsilon(h^4)\\
\phi_{x+h} &= \phi_O + h\left(\frac{\partial\phi}{\partial \mathrm{x}}\right)_O + \frac{h^2}{2!}\left(\frac{\partial^2\phi}{\partial \mathrm{x}^2}\right)_O + \frac{h^3}{3!}\left(\frac{\partial^3\phi}{\partial \mathrm{x}^3}\right)_O + \epsilon(h^4)\\
\phi_{y-h} &= \phi_O - h\left(\frac{\partial\phi}{\partial \mathrm{y}}\right)_O + \frac{h^2}{2!}\left(\frac{\partial^2\phi}{\partial \mathrm{y}^2}\right)_O - \frac{h^3}{3!}\left(\frac{\partial^3\phi}{\partial \mathrm{y}^3}\right)_O + \epsilon(h^4)\\
\phi_{y+h} &= \phi_O + h\left(\frac{\partial\phi}{\partial \mathrm{y}}\right)_O + \frac{h^2}{2!}\left(\frac{\partial^2\phi}{\partial \mathrm{y}^2}\right)_O + \frac{h^3}{3!}\left(\frac{\partial^3\phi}{\partial \mathrm{y}^3}\right)_O + \epsilon(h^4)
\end{aligned} \tag{32}$$

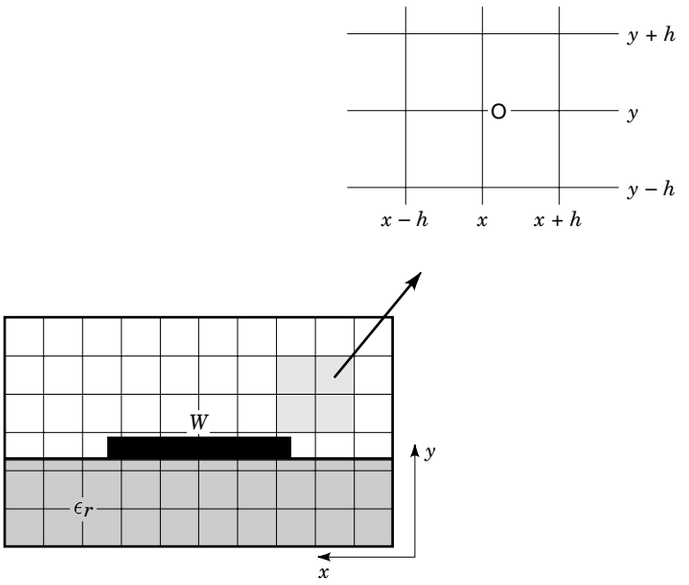

Figure 4. Finite difference discretization of a microstrip transmission line.

Where $\epsilon(h^4)$ is the remaining error. Adding these equations and considering that the resulting term

$$h^2\left(\frac{\partial^2\phi}{\partial x^2} + \frac{\partial^2\phi}{\partial y^2}\right)_O = 0$$

the approximation of ϕ_o at node center o becomes

$$\frac{1}{4}\left(\phi_{x+h} + \phi_{x-h} + \phi_{y+h} + \phi_{y-h}\right) = \phi_O$$

Whereby it is assumed that $\epsilon(h^4)$ is negligible. This equation shows that the value of ϕ_o is the average of the potentials at the four neighbouring points. The above equation for the 2-D problem is also said to be the five point difference equation of the Laplacian problem. For a 3-D problem the above equation expands to a seven-star node

$$\frac{1}{6}\left(\phi_{x+h} + \phi_{x-h} + \phi_{y+h} + \phi_{y-h} + \phi_{z+h} + \phi_{z-h}\right) = \phi_O$$

Repeating this procedure over the whole computational domain and considering the boundary conditions on ϕ, leads to the following matrix equation

$$[A]\mathbf{f} = \mathbf{X}$$

Since the individual grid points are only connected to their neighboring points, the coefficient matrix $[A]$ contains a large number of zero elements (banded sparse matrix) and only the diagonal and nearby elements are filled. $\mathbf{f}$ is a vector of all potentials on the interior nodes and $\mathbf{X}$ contains the information about the boundary conditions (or sources). Matrix $[A]$ can be solved by the Gauss-elimination method but due to the sparsity of the matrix, iterative methods such as the overrelaxation iteration are more economical in terms of computer resources.

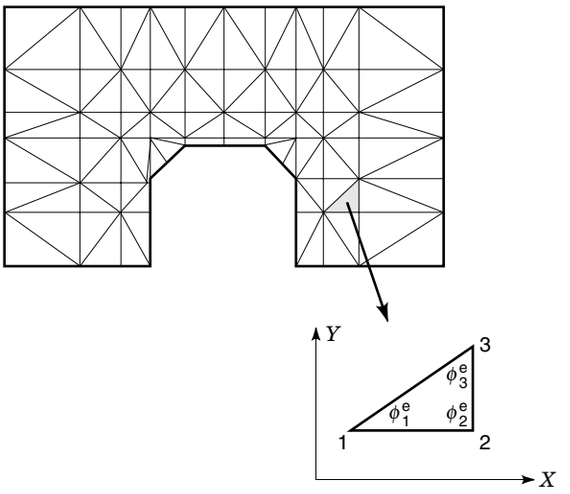

Figure 5. Finite-element discretization of a ridged waveguide.

Finite-Element Method

Although the finite-element method (FEM) was used by mechanical and civil engineers for many years (27), its application to the electromagnetics area was not before 1967 by Winslow (28) and in 1970 by Silvester and co-workers (29). Since then, the FEM has become a widely used numerical simulation tool for electromagnetic fields in structures with arbitrary boundary shape (30,31). In contrast to the finite-difference method, the finite element method discretizes the computational domain with a number of small interconnected subregions, called elements (Fig. 5). The shape of these elements is typically rectangular or triangular. This explains why there are virtually no restrictions on the shape of the structures that can be analyzed with the FEM. This feature is its main advantage over other methods.

The FEM is based on the fact that the potential function ϕ^e (superscript e denotes 'element') within each element, can be approximated by an (often linear) interpolation function which is zero outside the element. Summation of ϕ^e over all elements N gives an approximate solution for the total potential in the computational domain

$$\phi = \sum_p^N \phi^e(x, y) \tag{33}$$

The simplest form of approximation for ϕ^e within a triangular element (Fig. 5) is the following:

$$\phi^e = a + bx + cy \tag{34}$$

It is assumed that the field strength is uniform within a small element and that the potential varies linearly depending on the coordinates x and y. The unknown parameters a, b, c are found from the nodal parameters ϕ_p^e, x_p and y_p ($p = 1, 2, 3$) as

$$\begin{bmatrix} a \\ b \\ c \end{bmatrix} = \begin{bmatrix} 1 & x_1 & y_1 \\ 1 & x_2 & y_2 \\ 1 & x_3 & y_3 \end{bmatrix}^{-1} \begin{bmatrix} \phi_1^e \\ \phi_2^e \\ \phi_3^e \end{bmatrix} \tag{35}$$

Substituting the functions obtained from Eq. (35) into Eq. (34) yields

$$\phi^e = \sum_p N_p^e \phi_p^e \tag{36}$$

N_p^e are the so-called shape functions. The potential ϕ^e within each element is thus a linear combination of the shape functions and the three nodal values of the triangle.

The next step in the FEM is to determine the potential at the corners of all elements. This is usually done by minimizing (or maximizing) a functional that is known to be stationary about the true solution (variational method). For a Laplacian problem, the equivalent functional for each element is

$$I^e(\phi^e) = \int_{s^e} \frac{1}{2}\epsilon |\nabla \phi^e|^2 \, dx \, dy \tag{37}$$

The functional over all elements is then the sum over Eq. (37). From a physical point of view, I^e is the energy per unit length of the element e. Substituting the approximation for ϕ^e into Eq. (37) yields

$$I^e = \frac{1}{2} \sum_{p=1}^{3} \sum_{k=1}^{3} \epsilon \phi_p^e \underbrace{\left[\int_{s^e} \nabla N_p^e \cdot \nabla N_k^e \, dx \, dy \right]}_{C_{pk}} \phi_k^e \tag{38}$$

or in matrix form

$$I^e = \frac{1}{2} \epsilon [\phi^e]^T [C^e][\phi^e] \tag{39}$$

$[C^e]$ is the element coefficient matrix (stiffness matrix in structural analysis). The matrix elements represent the coupling between the nodes. Summation of Eq. (39) over all the elements and applying the extremum condition of the functional

$$\frac{\partial I(\phi)}{\partial \phi_i} = 0$$

yields the system matrix equation

$$[C][\phi] = 0 \tag{40}$$

$[C]$ is a sparse, symmetric and banded matrix of size $M \times M$ (M = total number of nodes). Equation (40) can be solved for the potentials of all nodes in the computational domain.

The FEM is one of the most flexible numerical modeling approaches which can be applied to nonlinear problems and also can be formulated in time and frequency domain. Although its formulation is more involved than the finite difference method the advantage of the FEM is that it can be applied to almost arbitrarily shaped boundaries. Application to open boundaries is difficult except if the FEM is combined with other methods which are more suitable for open boundary problems.

The Boundary-Element Method

The boundary-element method (BEM) or boundary integral element method is similar to the finite-element method applied to the boundary only. As such the BEM is also known

as a form of weighted residual technique that falls under the category of moment methods. The main advantage of the BEM over the FEM is that it reduces the dimension of the problem by one. For example, in a three-dimensional problem only the surface of the computational domain needs to be discretized and not the entire volume which leads to a much smaller number of algebraic equations. For two-dimensional problems the boundary elements are taken as straight line segments, whereas for three-dimensional problems triangular elements are taken. Disadvantages of the BEM are that the number of integrations required are great and that singularities must be considered. The calculation of the coefficient matrix may require more time than in the FEM.

A very detailed account of the BEM may be found in Ref. 2. In the BEM the quantity of interest ϕ anywhere within the computational domain is expressed in terms of a functional, except that this functional now depends only on the value of ϕ at the boundary and its normal derivative thereon. Again, for the Laplace equation in a source free volume Ω bounded by a surface Γ, for example, the potential ϕ_i inside the volume is given by the integral equation

$$\phi_i = \frac{1}{4\pi} \int_\Gamma \left[\frac{1}{r} \frac{\partial \phi}{\partial n} - \phi \frac{\partial}{\partial n} \left(\frac{1}{r} \right) \right] d\Gamma$$

In most of the relevant EM problems, the governing equation is not Laplace's and ϕ on the boundary is unknown. Then the boundary contour is discretized and ϕ for each boundary element is derived using the method of weighted residuals where the expansion and weighting functions are only defined within the boundary cell. The integral equation is thus transformed into a set of algebraic equations at the nodes of the boundary, and the value for ϕ and its derivatives are found simultaneously by solving a matrix equation (2).

TIME-DOMAIN METHODS

Time-domain methods are important if the time-domain response of an electromagnetic structure is required. Lately, time-domain methods have also gained momentum over frequency-domain methods since they deliver, depending on the excitation, all frequencies of interest with one computation run without the need for large matrix inversions. This feature is attractive if a wide band frequency response is required. One might also add that a variety of problems are more naturally formulated in the time domain than in the frequency domain. This is in particular the case for nonlinear problems.

Some of the frequency-domain methods discussed before can be formulated also in the time domain. This is a great advantage if one is already familiar with a particular method. Extending the formulation from one domain into the other without leaving the framework of one method not only minimizes the development effort but also expands the application range of that method. Among the many different techniques that can be formulated in both domains, the finite-difference time-domain (FDTD) method and the time-domain transmission line matrix (TDTLM) method are the most prominent ones. While the finite-difference method in the frequency domain, the FDM or FDFDM, has been discussed in a previous section, the frequency-domain version of the TLM method, the FDTLM method (32), is not discussed here. However, as in the framework of the finite-difference methods the duality between frequency- and time-domain methods exists also in the framework of the TLM method.

In the FDTD and TDTLM methods of electromagnetic modeling the continuous field functions that satisfy Maxwell's equations are approximated by samples of these functions defined only at discrete points in space and time. In the most general sense, FDTD and TLM belong to the method of moments (MOM) family. In FDTD the electromagnetic field is approximated by a set of local pulse functions in space and time, while in TLM it is expressed as a superposition of impulse waves traveling forward and backward along the coordinate directions, their sum yielding the electric and their difference the magnetic field values, respectively. Thus, FDTD is formulated in terms of total electric and magnetic field samples in discretized space, whereas the TLM formulation employs elementary incident and reflected waves traveling on a mesh of transmission lines (scattering formulation).

While both methods can be derived rigorously from Maxwell's equations using MOM formalism (33) a more intuitive approach which is also historically authentic will be used to formulate the basic FDTD and TLM algorithms. Their properties and associated errors will be discussed, and some recent variations will be mentioned.

Finite-Difference Time-Domain Method

The finite-difference time-domain (FDTD) scheme is obtained by replacing the partial derivatives (space *and* time) in Maxwell's curl equations by finite differences. The best approximation is obtained by central differencing (trapezoidal rule), resulting in an error that is proportional to the square of the space and time step (second-order accuracy).

The first FDTD formulation was proposed by Yee in 1966 (34) and subsequently applied and developed further by Taflove and Brodwin (35). Yee simply replaced the partial derivatives in Maxwell's curl equations by central finite differences. Weiland (36) derived an equivalent discretization approach using finite integration of Maxwell's equations in 1977. Figure 6 shows a unit FDTD cell (Yee cell) of a Cartesian space grid. Continuous space and time coordinates (x, y, z, t) are replaced by discrete coordinates $l\ \Delta x$, $m\ \Delta y$, $n\ \Delta z$, $k\ \Delta t$, where l, m, n, k are integers and Δx, Δy, Δz and Δt are the space and time steps. Note that the three electric field components are defined along the edges of the cell, while the magnetic field components are normal to the cell faces. The

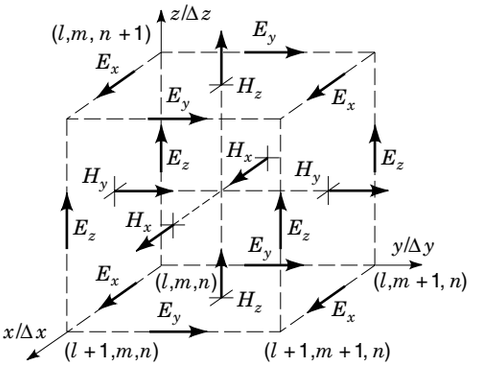

Figure 6. Topology of the elementary FDTD cell (Yee cell). Electric and magnetic field components are interleaved in space and time.

staggering of the field components by one-half of the cell dimensions is due to the central difference approximation of the differential operators. For the same reason, electric and magnetic field components are also staggered in time, the electric field components being defined at time points $k\ \Delta t$ and the magnetic field components at $[k + (1/2)\ \Delta t$.

If we assume that $\Delta x = p\ \Delta l$; $\Delta x = q\ \Delta l$; $\Delta x = r\ \Delta l$ where Δl is the unit reference length, and the scaling coefficients p, q, and r are all smaller or equal to unity, then the finite difference equations for the electric and magnetic field components in each cell are given by

$$
\begin{aligned}
{}_{k+1}E_x(l+\tfrac{1}{2},m,n) &= {}_kE_x(l+\tfrac{1}{2},m,n)+sx\{[{}_{k+1/2}H_z(l+\tfrac{1}{2},m+\tfrac{1}{2},n)\\
&\quad - {}_{k+1/2}H_z(l+\tfrac{1}{2},m-\tfrac{1}{2},n)]/q+[{}_{k+1/2}H_y(l+\tfrac{1}{2},m,n-\tfrac{1}{2})\\
&\quad - {}_{k+1/2}H_y(l+\tfrac{1}{2},m,n+\tfrac{1}{2})]/r\}\\
{}_{k+1}E_y(l,m+\tfrac{1}{2},n) &= {}_kE_y(l,m+\tfrac{1}{2},n)+sy\{[{}_{k+1/2}H_x(l,m+\tfrac{1}{2},n+\tfrac{1}{2})\\
&\quad - {}_{k+1/2}H_x(l,m+\tfrac{1}{2},n-\tfrac{1}{2})]/r+[{}_{k+1/2}H_z(l-\tfrac{1}{2},m,n+\tfrac{1}{2},n)\\
&\quad - {}_{k+1/2}H_z(l+\tfrac{1}{2},m+\tfrac{1}{2},n)]/p\}\\
{}_{k+1}E_z(l,m,n+\tfrac{1}{2}) &= {}_kE_z(l,m,n+\tfrac{1}{2})+sz\{[{}_{k+1/2}H_x(l,m-\tfrac{1}{2},n+\tfrac{1}{2})\\
&\quad - {}_{k+1/2}H_x(l,m+\tfrac{1}{2},n+\tfrac{1}{2})]/q+[{}_{k+1/2}H_y(l+\tfrac{1}{2},m,n+\tfrac{1}{2})\\
&\quad - {}_{k+1/2}H_y(l-\tfrac{1}{2},m,n+\tfrac{1}{2})]/p\}\\
{}_{k+1/2}H_x(l,m+\tfrac{1}{2},n+\tfrac{1}{2}) &= {}_{k-1/2}H_x(l,m+\tfrac{1}{2},n+\tfrac{1}{2})\\
&\quad + sx'\{[{}_kE_y(l,m+\tfrac{1}{2},n+1) - {}_kE_y(l,m+\tfrac{1}{2},n)]/p\\
&\quad + [{}_kE_z(l,m,n+\tfrac{1}{2}) - {}_kE_z(l,m+1,n+\tfrac{1}{2})]/q\}\\
{}_{k+1/2}H_y(l+\tfrac{1}{2},m,n+\tfrac{1}{2}) &= {}_{k-1/2}H_y(l+\tfrac{1}{2},m,n+\tfrac{1}{2})\\
&\quad + sy'\{[{}_kE_x(l+\tfrac{1}{2},m,n) - {}_kE_x(l+\tfrac{1}{2},m,n+1)]/r\\
&\quad + [{}_kE_z(l+1,m,n+\tfrac{1}{2}) - {}_kE_z(l,m,n+\tfrac{1}{2})]/p\}\\
{}_{k+1/2}H_z(l+\tfrac{1}{2},m+\tfrac{1}{2},n) &= {}_{k-1/2}H_z(l+\tfrac{1}{2},m+\tfrac{1}{2},n)\\
&\quad + sz'\{[{}_kE_x(l+\tfrac{1}{2},m+1,n) - {}_kE_x(l+\tfrac{1}{2},m,n)]/q\\
&\quad + [{}_kE_y(l,m+\tfrac{1}{2},n) - {}_kE_y(l+1,m+\tfrac{1}{2},n)]/r\}
\end{aligned}
\tag{41}
$$

where

$$
\begin{aligned}
sx &= Z_0 c\Delta t/(\epsilon_{rx}\Delta l)\\
sy &= Z_0 c\Delta t/(\epsilon_{ry}\Delta l)\\
sz &= Z_0 c\Delta t/(\epsilon_{rz}\Delta l)\\
sx' &= c\Delta t/(\mu_{rx}Z_0\Delta l)\\
sy' &= c\Delta t/(\mu_{ry}Z_0\Delta l)\\
sz' &= c\Delta t/(\mu_{rz}Z_0\Delta l)
\end{aligned}
\tag{42}
$$

In these expressions, c and Z_o are the velocity of light and the wave impedance *in vacuo,* and ϵ_{rx}, ϵ_{ry}, ϵ_{rz} and μ_{rx}, μ_{ry}, μ_{rz} are the diagonal elements of the relative permittivity and permeability tensors of the medium, respectively. This algorithm explicitly updates each field component in a leapfrog time-stepping process. The change in each E-field component is computed from the four H-field components circulating around it, and vice versa.

Stability. The process is stable as long as the time step is smaller than a maximum value known as the so-called Courant stability limit. For electrically and magnetically isotropic media characterized by ϵ_r and μ_r the stability criterion is:

$$
\Delta t \le \frac{\Delta l\sqrt{\mu_r\epsilon_r}}{c\sqrt{\dfrac{1}{p^2}+\dfrac{1}{q^2}+\dfrac{1}{r^2}}} \tag{43}
$$

Since in anisotropic media the wave velocity depends on the (generally unknown) polarization, it is prudent to enter the smallest of the three μ- and ϵ-values of the diagonal tensors into the stability condition. For free space discretized into cubic cells ($\mu_r = \epsilon_r = p = q = r = 1$) it becomes:

$$
\Delta t \le \frac{\Delta l}{c\sqrt{3}} \tag{44}
$$

Initial and Boundary Conditions. At the start of a computation the initial values of all electric and/or magnetic field components in the computational domain are specified before the updating process can begin. By enforcing the field values in certain regions at each time step, source functions with arbitrary time and space dependence can be modeled.

Boundary conditions must be enforced at each time step as well. Electric and magnetic walls are modeled by extending the discretized space one cell beyond the boundary and imposing appropriate symmetry conditions upon the field values on each side of the boundary. For example, the tangential electric field components must be identical on either side of a magnetic wall (ideal open circuit) and equal and opposite on either side of an electric wall (ideal short circuit). A dual condition applies to the tangential magnetic field components. Lossy resistive boundary conditions call for a fixed ratio between the tangential electric and magnetic field components at the boundary. More complex boundary conditions such as wide band absorbing walls or frequency dispersive boundaries call for special algorithms, such as one-way absorbing boundary conditions (37,38) or Berenger's perfectly matched layer (39). A detailed discussion of absorbing boundary conditions in FDTD and TLM can be found in Ref. 40. Similar approaches are required for the modeling of complex materials and devices.

The books by Kunz and Luebbers (41) and Taflove (42) are excellent sources of information on all aspects of FDTD modeling and contain extensive bibliographies on the theory, implementation and application of the FDTD method. Together with Yee's seminal paper (34) they are good starting points for exploring the extensive literature on FDTD theory and applications.

Transmission Line Matrix Method

The Expanded Node. The transmission line matrix (TLM) formulation of Maxwell's equations was first proposed in 1971 by Johns and Beurle (43). In their seminal paper they describe a novel numerical technique for solving two-dimensional scattering problems. Inspired by earlier network simulation techniques (44), they employ a Cartesian mesh of shunt-connected two-wire transmission lines as a discretized 2-D propagation medium. The nodes of this mesh act as scat-

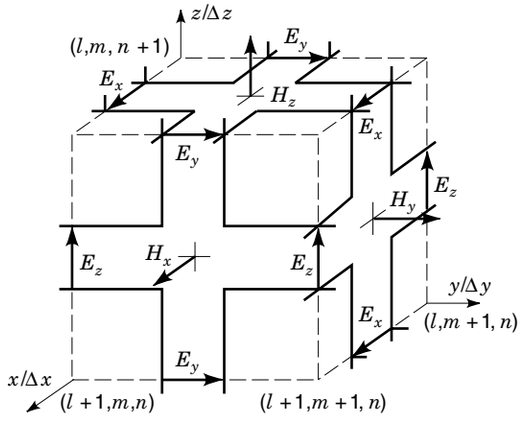

Figure 7. Topology of the expanded TLM node. Electric field components are modeled by the voltage across shunt connections, while magnetic field components are modeled by the loop current in series connections of transmission lines. The positions of the field components in space and time are identical to those in the Yee cell.

tering centers for short voltage impulses. Johns and Akhtarzad (45) extended the method to three space dimensions (the expanded node TLM model) in 1974, by creating an intricate 3-D lattice of shunt- and series-connected transmission lines, as shown in Fig. 7. This model is, in many respects, similar to the Yee cell in Fig. 6 since it yields identical solutions for the six field components when the time step in the Yee algorithm is set to $\Delta t = \Delta l/(2c)$ (free space, cubic cell). However, in contrast to the strictly mathematical formulation of FDTD, the TLM model is a "hardwired" network (albeit conceptual rather than material) to which all known techniques of circuit and transmission line analysis can be applied, both in frequency and time domains.

The Symmetrical Condensed Node. One of the shortcomings of these algorithms resides in the complicated topology of their unit cells and in the separate locations of electric and magnetic field components in space and time. This makes the modeling of complex boundary conditions and interfaces between materials more difficult and may introduce errors. To overcome these drawbacks, Johns (46,47) introduced the symmetrical condensed TLM node in 1986. This spawned the development of several new TLM formulations, from the hybrid and super condensed nodes to the alternating and rotated alternating (48) TLM models. In the following, the basic formulation proposed by Johns will be outlined. However, the port numbering scheme proposed by Russer (49) will be used since it allows a simpler and more compact representation of the TLM algorithm than Johns' original numbering scheme.

The Symmetrical Condensed Node TLM Algorithm. A unit cell of the symmetrical condensed TLM model is shown in Fig. 8. It contains a hybrid junction of twelve transmission lines (the node) which is characterized by a 12×12 scattering matrix. The time domain TLM algorithm is executed in two steps. Firstly, twelve short voltage pulses are simultaneously injected into the node ports 1 to 12. The pulses are scattered and give rise to twelve reflected voltage pulses. Secondly, the reflected pulses are transferred to the neighboring nodes where they become incident pulses at the subsequent time step, and the process is repeated. This series of events can be described in symbolic form as follows:

$$[{}_k v^r] = S \cdot [{}_k v^i], \qquad [{}_{k+1} v^i] = C \cdot [{}_k v^r] \tag{45}$$

where $[{}_k v^r]$ and $[{}_k v^i]$ are the vectors of reflected and incident pulses at the kth time step, $\boldsymbol{S}$ is the impulse scattering matrix of the node, and $\boldsymbol{C}$ is a connection matrix describing the topology of the network. It governs the transfer of the reflected pulses to the connected ports of the neighboring cells and/or the reflection from boundaries. The subscripts k and $k + 1$ denote the discrete time points at which the pulses are scattered at the nodes.

For a homogeneous, lossless, and isotropic medium, all transmission lines of a cubic cell have the same characteristic impedance. The 12×12 scattering matrix $\boldsymbol{S}$ is then

$$\boldsymbol{S} = \begin{bmatrix} 0 & \boldsymbol{S}_0 & \boldsymbol{S}_0^T \\ \boldsymbol{S}_0^T & 0 & \boldsymbol{S}_0 \\ \boldsymbol{S}_0 & \boldsymbol{S}_0^T & 0 \end{bmatrix} \tag{46}$$

where the submatrix $\boldsymbol{S}_0$ is given by

$$\boldsymbol{S}_0 = \begin{bmatrix} 0 & 0 & \frac{1}{2} & -\frac{1}{2} \\ 0 & 0 & -\frac{1}{2} & \frac{1}{2} \\ \frac{1}{2} & \frac{1}{2} & 0 & 0 \\ \frac{1}{2} & \frac{1}{2} & 0 & 0 \end{bmatrix} \tag{47}$$

Since the transit time Δt of the pulses is linked to the space step Δl by the pulse propagation velocity along the transmission lines, the TLM process is unconditionally stable. The time step is automatically set to $\Delta t = \Delta l/(2c)$.

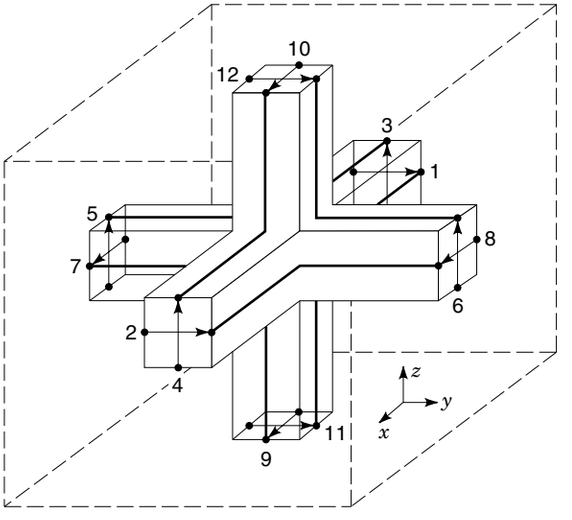

Figure 8. Topology of the symmetrical condensed TLM node. All six electric and magnetic field components are defined in the center of the node, and tangential field components are defined in the cell boundaries as well.

Inhomogeneous Materials and Losses. Dielectric or magnetic materials can be modeled by loading the nodes situated inside these materials with reactive shunt stubs of appropriate normalized characteristic admittance and a length $\Delta l/2$ (46). An open-circuited shunt stub will produce the effect of additional capacitance at the node, while a short-circuited series stub creates additional inductance. The resulting storage of reactive energy reduces the phase velocity and alters the intrinsic impedance in the structure. The interface conditions at the boundary between different materials are automatically fulfilled. Each cell can have a different set of stubs, (three permittivity and three permeability stubs) thus allowing the modeling of inhomogeneous anisotropic materials with diagonal permittivity and permeability tensors. The six stubs add six more ports to the node, and as a result, the $\boldsymbol{S}$ becomes an 18×18 matrix. Losses can be modeled by connecting so-called loss stubs to the nodes. The loss stubs are matched transmission line sections that extract a fraction of the energy scattered at the node at each time step. Since no pulses travel back into the nodes on these stubs, they only modify the elements of $\boldsymbol{S}$ without increasing its size.

Initial and Boundary Conditions. At the start of a computation the initial values of all pulses incident on all field components are uniquely determined in the center of the nodes by a linear combination of these pulses at the moment of scattering (47). When the pulses transit from one cell to the next ($t/\Delta t = k + 1/2$) the tangential components of the fields are obtained in the cell boundaries as well. By enforcing the pulse values (and hence the corresponding electric and magnetic field values) in certain regions at each time step, source functions with arbitrary time and space dependence can be modeled.

Boundary conditions can be imposed either in the center of the nodes or in the cell boundaries. In the latter case, boundaries are represented by means of impulse reflection coefficients. Electric walls reflect pulses with 'a -1' reflection coefficient, while magnetic walls have 'a $+1$' reflection coefficient. Lossy resistive boundaries have impulse reflection coefficients less than unity in magnitude. More complex boundary conditions such as wide band absorbing walls or frequency dispersive boundaries are treated in the same way as FDTD boundaries with the difference that the boundary operators are applied to the incident pulses rather than to the field quantities at the boundaries. It is straightforward to implement nonrecursive and recursive convolution techniques for the modeling of frequency dispersive boundaries and for partitioning large computational domains using time domain diakoptics (49). Similar approaches are required for the modeling of complex materials and devices (50).

Johns' seminal papers (43,45–47) are good starting points for exploring the world of TLM modeling, as are an introductory chapter on TLM by Hoefer (51) and a book by Christopoulos (52). They contain many references and describe the implementation and applications of TLM in detail.

HYBRID METHODS

None of the previous methods is capable of solving all electromagnetic modeling problems. The methods are either limited by the available computer memory and/or by computer run time, or the numerical model can simply not be applied to the structure at hand. For example, the method of moments is not applicable to structures with inhomogeneous or nonlinear dielectrics. The finite difference method is difficult to implement when fine circuit details must be resolved within a structure of large dimensions. The discretization size chosen for the smallest circuit detail determines the total number of discretization cells and thus the total matrix size to be handled may become too large. This problem is even more pronounced for the time domain version of the finite difference method, the FDTD, since here also the time is discretized. Similarily, the finite element method cannot efficiently model large radiation problems because of the large computational space that must be discretized.

In practice, many of these—and more—complicating factors are encountered. Not all appear in the same problem and at the same time, thus making it possible to choose one electromagnetic modeling approach over the other. But there is a significant number of problems (and others are emerging) that can not be solved within the framework of any of the previous methods.

A solution to those problems is possible by combining two or more techniques. The task is to apply each method to the problem domain for which it is best suited. There are two possible approaches. A two or more step procedure is utilized in which one part of the problem is solved by one method and the results are used as input data to solve remaining parts of the problem with other techniques. That requires that boundary conditions are established that must be enforced at the interfaces between the different regions. This approach is called an explicit hybrid approach. An implicit hybrid approach is one in which the advantageous features of one technique are combined with those of another technique to form a new stand-alone algorithm.

Several successful implementations of hybrid methods have been reported in the literature. Although this research direction does not replace the effort to improve existing single methods, hybrid methods offer electromagnetic modeling of a whole new class of problems and may in particular be important in the area of CAD.

Combinations of Frequency-Domain Methods

GTD and MOM. The first combinations of electromagnetic modeling approaches appeared in the analysis of antenna problems and radar cross-sections. The geometrical theory of diffraction (GTD) and the method of moments were used to analyze antenna problems in Ref. 53. The GTD is an extension to geometric optics which includes the effect of diffraction. This method is only accurate if the dimensions of the object being analyzed is large compared to the wavelength of the field. For that reason this method is also called high-frequency method. In the combination of the GTD and the MOM, the latter is used to solve the region close to the antenna, while the GTD is used for the free space surrounding the antenna.

FEM and GSM Technique. A combination of the finite-element method (FEM) and the generalized scattering matrix (GSM) technique was utilized in the study of scattering from jet engines (54). The FEM was applied to the complex part of the scatterer to generate the GSM at its boundary which can

then be interfaced with high frequency techniques for computation of the engine's scattered fields without reference to the geometry of the jet engine. One of the methods alone would not have been able to solve this complex problem.

FEM/FDM and MMT. For the analysis of microwave circuits the combination of the FEM and the mode matching technique (MMT) has been proposed to study large cavities (55). In Ref. 56 the FEM was applied to analyze waveguide discontinuities with arbitrary boundary shape. In Ref. 57 the FDM was employed instead of the FEM to analyze segments of waveguide structures that are not suitable for a MMT analysis, for example a circular stub in a rectangular waveguide. In all these papers the MMT was used to characterize the uniform sections of the waveguide while the FEM or FDM was employed to analyze rounded corners or discontinuity shapes that do not fit into the coordinate system of the MMT. The latter was then used to derive the scattering parameters of the overall circuit.

Method of Lines and SDM. For the 3-D analysis of planar waveguide problems a combination of the method of lines and the spectral domain method was introduced in Ref. 58. The purpose of this combination was to eliminate some of the problems associated with the 2-D MOL and the 2-D SDM. The problem in the latter was the difficulty to find 2-D basis functions which converge easily, while for the 2-D MOL a 2-D discretization may not always be able to satisfy all boundary conditions simultaneously with effortable computer memory. The combination of the computationally very efficient 1-D SDM in transverse direction of the propagating wave with the equally efficient 1-D MOL in propagation direction eliminates these problems.

Combinations of Time- and Frequency-Domain Methods

Hybrid Finite-Difference Time-Domain Method. The hybrid finite-difference time-domain (HFDTD) method is a combination of frequency-domain and time-domain concepts. In its widest sense, the technique utilizes a standard FDTD mesh in the areas of structure inhomogenouity and expansion into a known set of modes in transversely homogeneous regions of the structure. This provides substantial savings both in terms of computer memory and CPU-time as was first demonstrated in the eigenvalue analysis of planar transmission lines (60). A conventional FDTD analysis of such a structure requires a 3-D mesh which, depending on the space resolution required, needs several thousand time iterations before a Fourier transform can provide the results for the propagation constant. By replacing the space discretization in propagation direction (z) by a simple phase shift (note that the field at location l_z is different from that at location $l_z + z$ by only a factor $e^{-j\beta z}$), results in a 2-D FDTD mesh (59). Multiplying the field equations furthermore by a factor j such that

$$E_x, E_y, H_z = j(E_x, E_y, H_z)e^{-j\beta z}$$
$$H_x, H_y, E_z = (H_x, H_y, E_z)e^{-j\beta z}$$

leads to discretized Maxwell's equations without complex quantities. This feature accelerates the computation considerably. Exciting the 2-D mesh with a time domain impulse requires much less time iterations for the impulse to settle than in the case of a 3-D mesh. A Fourier transform provides the frequency at which the assumed value of β is valid.

The same principle can be applied to the time domain TLM method and also here significant savings in computer resources are possible if only the propagation constant and related quantities (characteristic impedance, losses) are of interest.

TDTLM and MMT. In the TDTLM analysis of complex cascaded discontinuity problems, diakoptics is used to subdivide the problem into simpler subsections which are then modelled individually. Interconnecting the individual solutions requires a node to node convolution at the interface. This approach tends to be computationally quite demanding since the number of convolutions increases with N^2 (N is the number of branches of interest). To reduce the computational effort, it was suggested in Ref. 61 that the uniform sections of the problem domain are modelled by modal functions treated in the time domain (time domain Green's function), while the discontinuity region is represented by the TDTLM method for which the incident fields are superpositions of those modes. The response of that subvolume to an excitation is obtained by convolution of the excitation with the time domain Green's function. This approach leads to a significant reduction of the computational resources as compared to the analysis with only the TDTLM. Furthermore, the complex discontinuity region is now represented by its generalized scattering matrix (GSM) which makes it easy to cascade discontinuities.

Combinations of Time-Domain Methods

FDTD and FEM. The FDTD method is well suited for applications in Cartesian coordinates. However, as soon as mixed coordinates are necessary to describe the problem contour, a staircase approximation must be utilized. For example, a round structure within a rectangular mesh layout can only be described accurately by a fine staircase approximation. This leads to a very fine mesh and consequently a small time step to satisfy the stability condition. The computational effort to calculate such a structure with acceptable accuracy becomes prohibitive. An alternative solution is to model the arbitrary boundary with the finite element method and incorporate this approach in the FDTD method which is applied elsewhere in the problem domain (62).

The list of methods that have been combined can be continued and new combinations appear every month in the various periodicals. A good starting point to find out more about hybrid methods and the rational behind their combinations is in Ref. 63.

SUMMARY

The tremendous increase of computer power over the last ten years has inspired a new era in the field of electromagnetic modeling or computational electromagnetics. Numerical codes that ran only on super-computers yesterday are running on workstation computers today. This development will not stop here and the electromagnetic modeling problem that appears to be inaccessible by any of today's available codes (because the required computer resources are just too large) will be solvable with tomorrow's computers and the then available (unlimited?) computer memory.

Because of this rapid development in computer hardware, electromagnetic modeling has become a common place in the world of electrical engineers. Many of the methods that we have briefly described are already implemented in commercial simulation tools used in practice to analyze a wide variety of problems and to design (CAD) a wide range of circuits and components which would not function otherwise.

We have divided the methods into frequency-domain, time-domain, and hybrid methods. They all have advantages and disadvantages depending on the problem range they are applied to. The aim of this article was not to provide extensive information on all of these methods but to introduce the reader to those numerical methods that have a broad enough application as well as to provide key references for further reading.

FURTHER READING

The literature on electromagnetic field modeling is quite extensive and only a few key references could be cited here. For more information on the subject the reader is referred to the books by R. Sorrentino (64) and E. Miller et al. (65), who have assembled a collection of reprints of key papers on the subject, and the book by E. Yamashita (66). Furthermore, various journals and conferences are devoted to the topic of numerical modeling of electromagnetic fields.

BIBLIOGRAPHY

1. Sadiku, *Numerical Techniques in Electromagnetics,* Boca Raton, FL: CRC Press, 1992.
2. P. B. Zhou, *Numerical Analysis of Electromagnetic Fields,* New York: Springer Verlag, 1993.
3. T. Itoh, *Numerical Techniques for Microwave and Millimeter-Wave Passive Structures,* New York: Wiley, 1989.
4. G. S. Mikhlin, *Variational Methods in Mathematical Physics,* New York: Pergamon Press, 1968.
5. R. F. Harrington, *Field Computation by Moment Methods,* Malabar, FL: Krieger, 1968.
6. A. Wexler, Solution of waveguide discontinuities by modal analysis, *IEEE Trans. Microw. Theory Tech.,* **MTT-15**: 508–517, 1967.
7. Mittra and W. W. Lee, *Analytical Techniques in the Theory of Guided Waves,* New York: Macmillan, 1971.
8. R. Vahldieck, Accurate hybrid mode analysis of various finline configurations including multilayered dielectrics, finite metallization thickness and substrate holding grooves, *IEEE Trans. Microw. Theory Tech.,* **MTT-32**: 1454–1460, 1984.
9. R. R. Mansour and R. McPhie, A unified hybrid-mode analysis for planar transmission lines with multilayer isotropic/anisotropic substrates, *IEEE Trans. Microw. Theory Tech.,* **MTT-35**: 1382–1391, 1987.
10. Y. C. Shih, The mode-matching method, in T. Itoh (ed.), *Numerical Techniques for Passive Microwave and Millimeter-Wave Structures,* New York: Wiley, 1989, chap. 9.
11. J. Bornemann and F. Arndt, Modal s-matrix design of optimum, stepped, ridged and finned waveguide transformers, *IEEE Trans. Microw. Theory Tech.,* **MTT-35**: 561–567, 1987.
12. S. Amari, J. Bornemann, and R. Vahldieck, Accurate analysis of scattering from multiple waveguide discontinuities using the coupled-integral equation technique, *J. Electromagn. Waves Appl.,* **10**: 1623–1644, 1996.
13. S. Amari, J. Bornemann, and R. Vahldieck, Accurate and fast analysis of waveguide filters by the coupled-integral equation technique, *IEEE Trans. Microw. Theory Tech.,* **MTT-45**: 1611–1618, 1997.
14. Itoh and R. Mittra, Spectral-domain approach for calculating the dispersion characteristics of microstrip lines, *IEEE Trans. Microw. Theory Tech.,* **MTT-21**: 496–499, 1973.
15. T. Uwaro and T. Itoh, Spectral domain approach, in T. Itoh (ed.), *Numerical Techniques For Microwave and Millimeter-Wave Passive Structures,* New York: Wiley, 1989, chap. 5.
16. T. Kitazawa, Metallization thickness effect of striplines with anisotropic media: quasi-static and hybrid mode analysis, *IEEE Trans. Microw. Theory Tech.,* **MTT-37**: 769–775, 1989.
17. T. Kitazawa and R. Mittra, Analysis of finline with finite metallization thickness, *IEEE Trans. Microw. Theory Tech.,* **MTT-32**: 1484–1487, 1984.
18. A. Ludwig, A new technique for numerical electromagnetics, *IEEE AP-S Newslett.,* **31**: 40–41, February 1989.
19. Ch. Hafner and L. Bomholt, *The 3D Electrodynamic Wave Simulator,* New York: Wiley, 1993.
20. P. Leuchtmann, The multiple multipole program (MMP): theory, practical use and latest features, *ACES,* Mar. 1995. 121 pages, available from author, leuchtmann@ifh.ee.ethz.ch.
21. O. A. Liskovets, The method of lines, Review, *Diff. Uravneniya,* **1**: 1662–1678, 1965.
22. B. P. Demidowitsch et al., *Numerical Methods of Analysis,* Berlin: VEB Wissenschaften, 1968, chap. 5, in German.
23. R. Pregla and W. Pascher, The method of lines, in T. Itoh (ed.), *Numerical Techniques for Microwave and Millimeter—Wave Passive Structures,* New York: Wiley, 381–446, 1989, chap. 6.
24. S. Xiao, R. Vahldieck, and J. Hesselbarth, Analysis of cylindrical transmission lines with the method of lines, *IEEE Trans. Microw. Theory Tech.,* **MTT-44**: 993–999, 1996.
25. G. Mur, Finite difference method for the solution of electromagnetic waveguide discontinuity problem, *IEEE Trans. Microw. Theory Tech.,* **MTT-22**: 54–57, 1974.
26. H. E. Green, The numerical solution of some important transmission-line problems, *IEEE Trans. Microw. Theory Tech.,* **MTT-13**: 676–692, 1965.
27. O. C. Zienkiewicz and Y. K. Cheung, *The Finite Element Method in Structural and Continuum Mechanics,* London: McGraw-Hill, 1967.
28. A. M. Winslow, Numerical solution of the quasilinear poisson's equation in a nonuniform triangular mesh, *J. Comp. Phys.,* **2**: 149–172, 1967.
29. P. P. Silvester and M. V. K. Chari, Finite element solution of saturable magnetic field problems, *IEEE Trans. Power Appar. Syst.,* **PAS-89**: 1642–1651, 1970.
30. P. Silvester, Finite element analysis of planar microwave networks, *IEEE Trans. Microw. Theory Tech.,* **MTT-21**: 104–108, 1973.
31. B. M. A. Rahman, A. Fernandez, and J. Davie, Review of finite element methods for microwave and optical waveguides, *Proc. IEEE,* **79** (10): 1442–1448, 1991.
32. H. Jin and R. Vahldieck, The frequency-domain transmission line matrix method—A New Concept, *IEEE Trans. Microw. Theory Tech.,* **MTT-40**: 2207–2218, 1992.
33. M. Krumpholz, C. Huber, and P. Russer, A field theoretical comparison of FDTD and TLM, *IEEE Trans. Microw. Theory Tech.,* **MTT-43**: 1935–1959, 1995.
34. K. S. Yee, Numerical solutions of initial boundary value problems involving Maxwell's equations in isotropic media, *IEEE Trans. Antennas Propag.,* **AP-14**: 302–307, 1966.

35. A. Taflove and M. E. Brodwin, Numerical solution of steady-state electromagnetic scattering problems using the time-dependent Maxwell's equations, *IEEE Trans. Microw. Theory Tech.,* **MTT-23**: 623–630, 1975.
36. T. Weiland, A discretization method for the solution of Maxwell's equations for six-component fields, *Electron. Commun., AEÜ,* **31**: 116–124, 1977.
37. G. Mur, Absorbing boundary conditions for the finite-difference approximation of the time-domain electromagnetic field equations, *IEEE Trans. Electromagn. Compat.,* **EMC-23**: 377–382, 1981.
38. T. G. Moore et al., Theory and application of radiation boundary operators, *IEEE Trans. Antennas Propag.,* **AP-36**: 1797–1812, 1988.
39. J.-P. Berenger, A perfectly matched layer for the absorption of electromagetic waves, *J. Computat. Phys.,* **114**: 185–200, 1994.
40. C. Eswarappa and W. J. R. Hoefer, Absorbing boundary conditions for time-domain TLM and FDTD analysis of electromagnetic structures, *Electromagnetics,* **16** (5): 489–519, 1996.
41. K. S. Kunz and R. J. Luebbers, *Finite Difference Time Domain Method for Electromagnetics,* Boca Raton, FL: CRC Press, 1993.
42. A. Taflove, *Computational Electrodynamics, The Finite-Difference Time-Domain Method,* Norwood, MA: Artech House, 1995.
43. P. B. Johns and R. L. Beurle, Numerical solution of 2-dimensional scattering problems using a transmission-line matrix, *IEE Proc.,* **118**: 1203–1208, 1971.
44. G. Kron, Equivalent circuit of the field equations of Maxwell-I, *Proc. IEEE,* **32**: 289–299, 1944.
45. S. Akhtarzad and P. B. Johns, Solution of 6-component electromagnetic fields in three space dimensions and time by the T.L.M. method, *Electron. Lett.,* **10**: 535–537, 1974.
46. P. B. Johns, New symmetrical condensed node for three-dimensional solution of electromagnetic wave problems by TLM, *Electron. Lett.,* **22**: 162–164, 1986.
47. P. B. Johns, A symmetrical condensed node for the TLM method, *IEEE Trans. Microw. Theory Tech.,* **MTT-35**: 370–377, 1987.
48. P. Russer and B. Bader, The alternating transmission line matrix ATLM scheme, in *1995 IEEE MTT Int. Microw. Symp. Dig.,* Orlando, FL, 1995, pp. 19–21.
49. W. J. R. Hoefer, The discrete time domain Green's function or Johns Matrix—a new powerful concept in TLM, *Int. J. Num. Modelling,* **2**: 215–225,1989.
50. L. R. A. X. de Menezes and W. J. R. Hoefer, Modeling of general constitutive relationships in SCN TLM, *IEEE Trans. Microw. Theory Tech.,* **MTT-44**: 854–861, 1996.
51. W. J. R. Hoefer, The transmission line matrix, TLM method, in T. Itoh (ed.), *Numerical Techniques for Passive Microwave and Millimeter-Wave Structures,* New York: Wiley, 1989, chap. 8.
52. C. Christopoulos, *The Transmission-Line Modeling Method TLM,* Piscataway, NY: IEEE Press, 1995.
53. G. A. Thiele and T. H. Newhouse, A hybrid technique for combining moments method and geometrical theory of diffraction, *IEEE Trans. Antennas Propag.,* **23**: 62, 1975.
54. D. C. Ross, J. L. Volakis, and H. T. Anastassiu, Hybrid finite element-modal analysis of jet engine inlet scattering, *IEEE Trans. Antennas Propag.,* **43**: 277–285, 1995.
55. M. S. Tharf and G. I. Costache, Finite element solutions of field distributions in large cavities, *Int. J. Numerical Modeling Electron. Networks, Device Fields,* **7** (5): 343–356, 1994.
56. R. Beyer and F. Arndt, Efficient modal analysis of waveguide filters including the orthogonal mode coupling elements by an MM/FE method, *IEEE Microw. Guided Wave Lett.,* **5** (1): 1–3, 1995.
57. M. Mogiardo and R. Sorrentino, Efficient and versatile analysis of microwave structures by combined mode matching and finite difference methods, *IEEE Microw. Guided Wave Lett.,* **3** (8): 241–243, 1993.
58. K. Wu, M. Yu, and R. Vahldieck, Rigorous analysis of 3D planar circuit discontinuities using the space-spectral domain approach, *IEEE Trans. Microw. Theory Tech.,* **MTT-40**: 1475–1483, 1992.
59. S. Xiao and R. Vahldieck, An efficient 2-D FDTD algorithm using real variables, *IEEE Microw. Guided Wave Lett.,* **3**: 127–129, 1993.
60. F. Alimenti et al., Efficient analysis of waveguide components by FDTD combined with time domain modal expansion, *IEEE Microw. Guided Wave Lett.,* **5**: 351–353, 1995.
61. M. Righi and W. J. R. Hoefer, Efficient 3D-SCN-TLM diakoptics for waveguide components, *IEEE Trans. Microw. Theory Tech.,* **MTT-42**: 2381–2385, 1994.
62. R. Wu and T. Itoh, Hybridizating FDTD analysis with unconditionally stable FEM for objects with curved boundary, *1995 IEEE MTT Int. Microw. Symp. Dig.,* Orlando, FL, 1995, pp. 833–836.
63. Session on hybrid methods, *IEEE AP-S Int. Symp. Dig.,* Newport Beach, CA, June 1995, pp. 1456–1483.
64. E. Yamashita (Editor), *Analysis Methods for Electromagnetic Wave Problems,* Norwood, MA: Artech House, 1990.
65. R. Sorrentino (Editor), *Numerical Methods for Passive Microwave and Millimeter Wave Structures,* Piscataway, NJ: IEEE Press, 1989.
66. E. Miller, L. Medgyesi-Mitschang, and E. Newman, *Computational Electromagnetics,* Piscataway, NJ: IEEE Press, 1991.

R. VAHLDIECK
Swiss Federal Institute of Technology Zurich (ETHZ)

WOLFGANG J. R. HOEFER
University of Victoria